Calculation of 2D and 3D Phase Diagrams

SHUANGLIN CHEN,[1,2,4] WEISHENG CAO,[1] FAN ZHANG,[1]
QIAN LI,[2,3] JIEYU ZHANG,[2] CHUAN ZHANG,[1] and JUN ZHU[1]

1.—CompuTherm, LLC, Madison, WI 53719, USA. 2.—State Key Laboratory of Advanced Special
Steels, Shanghai University, Shanghai 200072, China. 3.—Institute of Genomic Material, Shanghai
University, Shanghai 200444, China. 4.—e-mail: Shuanglin.Chen@computherm.com

The algorithms for calculating two-dimensional (2D) phase diagrams and
three-dimensional (3D) phase diagrams are described. While the concept of
the zero-phase-fraction is used to calculate 2D phase diagrams, the concept of
one-phase fraction is applied to calculate 3D phase diagrams. 3D phase dia-
grams can be better viewed with contour lines such as isothermal lines on the
3D phase boundary surfaces. The concepts of zero-phase fraction and one-
phase fraction have also been generalized to a contour line of any property.

INTRODUCTION

Materials are the cornerstone of modern technol-
ogy. The materials community is facing the challenge
of designing new materials and improving existing
ones to meet the needs of new technologies. In order to
improve the efficiency of materials research, the
concept of integrated computational materials engi-
neering (ICME) has been proposed and applied in
both materials research and industrial applications.
There have been great achievements in ICME in the
past decade.[1,2] One of the important components in
ICME is the simulation of the variety of phase prop-
erties such as thermodynamic, kinetic and mechan-
ical. All phase-related properties are closely related
to phase equilibria, which can be presented graphi-
cally in phase diagrams.

Phase diagrams, often referred to as the road
maps of materials, have played a fundamental role
in materials design.[3] In the early days, most phase
diagrams were measured experimentally and lim-
ited to unary, binary and ternary systems.[4,5] Cal-
culation of phase diagrams can be dated back to van
Laar [6,7] and Meijering,[8] who calculated some simple
binary and ternary phase diagrams with miscibility
gaps. The 1970s marked the start of phase diagram
calculations with computers as a new materials re-
search method pioneered by Kaufman, et al.[9] who
then founded the CALPHAD journal. The CAL-
PHAD method has now become one of the important
simulation methods in ICME.

Phase diagrams are conventionally compiled in
handbooks.[5,10] With the availability of the internet,
many commonly used online phase diagrams are
now available online.[11–14] Phase diagrams in
handbooks and online databases are mostly two-di-
mensional (2D) static diagrams and limited to lower
order systems. However, the phase diagrams of
multi-components for practical applications are
usually not available in handbooks or online phase
diagram databases. In order to calculate multicom-
ponent phase diagrams that are technically useful,
both computer software and multicomponent ther-
modynamic databases are needed. In recent years,
several phase diagram calculation software, such as
Pandat, Thermo-Calc, and FACTSage, have been
developed for such a purpose. These software
packages have been reviewed in a special issue of
CALPHAD journal.[15]

A phase diagram is usually calculated and pre-
sented in a 2D space, in which two variables are
used. For a multi-component system, a 2D phase
diagram only provides partial phase equilibrium
information which can be presented on the defined
2D section. Therefore, a series of 2D diagrams are
needed for a better understanding of a multi-com-
ponent system. For example, a series of isothermal
and/or isoplethal sections are usually calculated to
reveal the phase equilibrium relationships in a
ternary system. Should a phase diagram be calcu-
lated and presented in a three-dimensional (3D)
space, more information on multi-component phase
equilibria can be viewed in a more intuitive way. In
fact, 3D phase diagrams are sometimes calculated.
A typical example is a ternary liquidus projection. A
liquidus projection is calculated in a 3D space with
temperature and two compositional variables, but
projected in a 2D space. The first-melting projection

diagram presented recently by Eriksson et al.[16] is a special type of 3D phase diagrams.

Along with the advancement of the computer technology, such as advanced algorithms and graphic tools, it is now possible to calculate a 3D phase diagram directly using phase diagram calculation software. Recently, the 3D phase diagram calculation function has been implemented in Pandat software. In this paper, we will first describe the algorithm used for calculating a 2D phase diagram and then proceed to the 3D ternary liquidus projection. The algorithm for calculating a liquidus projection will be extended for the calculation of a full 3D phase diagram.

2D PHASE DIAGRAM

A 2D phase diagram has a unique property as pointed out by Morral et al.[17,18] This unique property states that each phase boundary in a 2D phase diagram corresponds to a zero-phase-fraction (ZPF) of a specific phase. Figure 1 is a simple isothermal section for a hypothetical ternary A–B–C system and is used here to illustrate the concept of ZPF.

In Fig. 1, the A–B–C system at a given temperature has seven phase regions, α, β, γ, $\alpha + \beta$, $\alpha + \gamma$, $\beta + \gamma$ and $\alpha + \beta + \gamma$, which are separated by nine phase boundaries. A phase boundary between a single-phase region and a two-phase region has the property of one phase with a fraction of one and the other with zero. For example, the boundary ad separates the phase regions of α and $\alpha + \beta$ and it has $f^\alpha = 1$ and $f^\beta = 0$. A phase boundary between a two-phase region and a three-phase region has the

property that one phase has a phase fraction of zero and the other two phases have phase fractions varying from zero to one. For example, boundary ac separates the two-phase region $\alpha + \gamma$ and the three-phase region $\alpha + \beta + \gamma$, and it has $f^\beta = 0$ and $0 \le f^\alpha \le 1$, $0 \le f^\gamma \le 1$. Examining other phase boundaries shows that each boundary has a characteristic property that one phase always has the phase fraction of zero on the boundary. This conclusion can be extended to any 2D section phase diagrams. In Fig. 1, the three boundaries eb, bc and ch have $f^\alpha = 0$ and form the ZPF line ebch of the phase α, which is colored red. The ZPF line ebch divides the compositional triangle into two parts. On one side of ebch (above), α phase is stable and has $f^\alpha > 0$, while on the other side of ebch, α phase is not stable and has $f^\alpha = 0$. Similarly, the ZPF of β phase is dacg (green color) and the ZPF of γ phase is iabf (magenta color). Therefore, a 2D phase diagram can be viewed as an overlap of stable phase regions.

With the concept of ZPF lines in a 2D phase diagram, it is straightforward to calculate the 2D phase boundaries. The commonly used algorithm for calculating a 2D phase diagram is based on this ZPF property and calculates the phase equilibria on every boundary with the ZPF constraint of a specific phase. For example, the phase boundary ab in Fig. 1 is calculated with the following equations,

$$\mu_i^\alpha = \mu_i^\beta = \mu_i^\gamma \quad (i = A, B, C) \tag{1}$$

$$f^\gamma = 0 \tag{2}$$

Similar equations could be written for the other phase boundaries according to the phases in equilibrium.

LIQUIDUS PROJECTION

At constant pressure, a ternary liquidus projection can be viewed as a special type of 2D phase diagram. The liquidus surface is actually a 3D surface in the space of $T–x_2 - x_3$ (x_1 is considered as a dependent composition variable). When a 3D liquidus surface is projected along the temperature direction onto the compositional 2D plane, it becomes a 2D liquidus projection on the plane of $x_2 - x_3$. Figure 2a is the liquidus surface of a ternary system A–B–C, and Fig. 2b is its projection on $x_C - x_A$. It has three ternary liquidus lines ae, be and ce, and they meet at the ternary eutectic point e. Isothermal lines are also calculated and their temperatures are labeled beside the lines.

In principle, a liquidus projection is composed of the liquidus phase boundaries in a series of 2D isothermal sections. As long as those isothermal sections are calculated, a careful combination of the liquidus boundaries will form the ternary liquidus lines as well as the isothermal lines. However, this
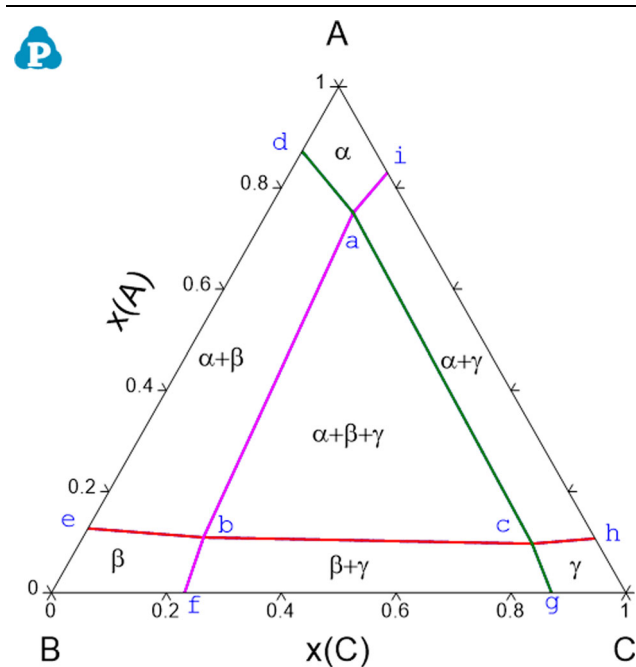

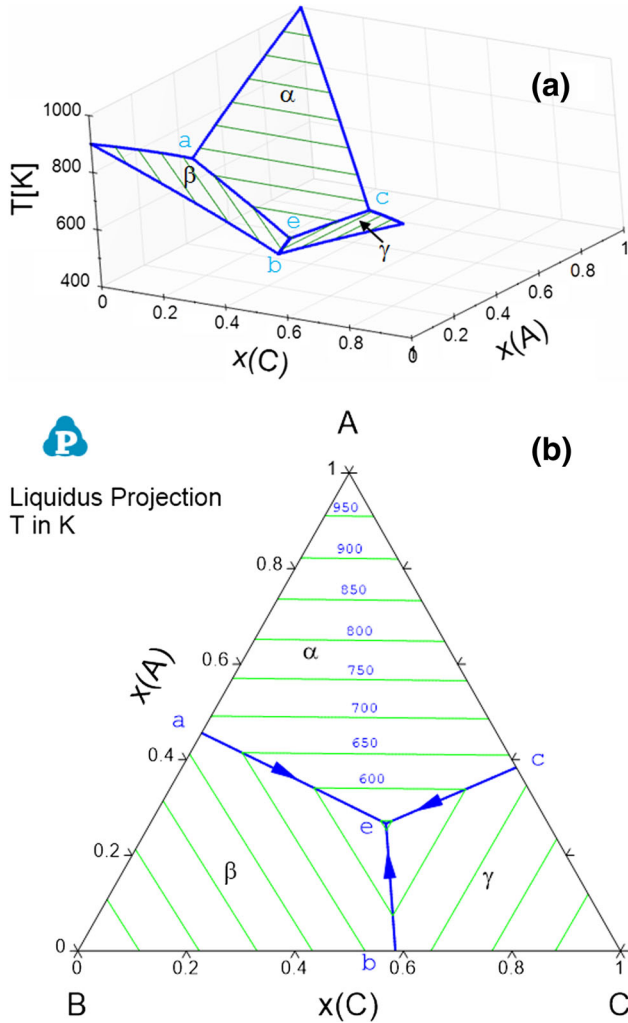Fig. 1. Isothermal section for a hypothetical system A–B–C.

Fig. 2. (a) Liquidus surface, (b) liquidus projection of ternary A–B–C with isothermal lines.

$$\mu_i^L = \mu_i^\alpha = \mu_i^\beta \quad (i = A, B, C) \qquad (3)$$

$$f^L = 1 \qquad (4)$$

A point on any isothermal line in the α primary phase region in Fig. 2 can be calculated with these equations,

$$\mu_i^L = \mu_i^\alpha \quad (i = A, B, C) \qquad (5)$$

$$f^L = 1 \qquad (6)$$

$$T = T^* \qquad (7)$$

where T^* is the temperature of the isothermal line where the point is to be calculated.

3D PHASE DIAGRAM

Ternary 3D phase diagrams were vividly drawn in the classic textbook *Phase Diagrams in Metallurgy* by Rhines.[19] Recently, Pandat software implemented a function to calculate 3D phase diagrams directly.[20] The algorithm of calculating liquidus surface presented in the previous section can be extended to calculate a full 3D phase diagrams including those phase boundaries among the solid phases. Figure 3a shows the calculated 3D phase diagram of a hypothetical system, A–B–C. The following equations are used to calculate the 3D univariant line on the surface of α phase in equilibrium with β and γ,

$$\mu_i^\alpha = \mu_i^\beta = \mu_i^\gamma \quad (i = A, B, C) \qquad (8)$$

$$f^\alpha = 1 \qquad (9)$$

These set of equations will calculate the edges α_1–α_2 of the α phase region, as shown in Fig. 3b. Change to different sets of the phases in Eqs. 8 and 9 will calculate other univariant edges in the 3D phase diagram.

To have a better view of a 3D diagram, contour lines on the 3D surfaces are needed. In this ternary A–B–C system, the isothermal lines on the 3D boundaries of the solidus surfaces will be the best contour lines. The equations of the isothermal lines on the α solvus surface in equilibrium with β phase are listed below,

$$\mu_i^\alpha = \mu_i^\beta \quad (i = A, B, C) \qquad (10)$$

$$f^\alpha = 1 \qquad (11)$$

algorithm is not efficient because the calculation of non-liquidus boundaries is not necessary and the combination of liquidus boundaries may need extra work near the binary and ternary invariant points on the liquidus surface. A different algorithm should work better for the liquidus surface.

A careful examination on the liquidus surface and projection reveals that all the points on the liquidus surface have a unique property, i.e., the fraction of the liquid phase is always one. Thus, a liquidus projection diagram is different from the 2D section diagrams. The fraction of liquid phase on the univariant liquidus valley lines and the isothermal lines is one, while those of the other phases are zero. It should be pointed out that the other phase can be liquid if the liquid exhibits a miscibility gap. With this unique characteristic property, a liquidus surface diagram can be calculated. For example, a point on the univariant liquidus line ae can be calculated from the following equations:

Changing the set of phases in above equations, we will be able to calculate the isothermal lines on other phase boundary surfaces.

For the ternary invariant reaction, i.e., the ternary four-phase eutectic reaction among L, α, β and γ in this example, the equations are

$$\mu_i^L = \mu_i^\alpha = \mu_i^\beta = \mu_i^\gamma \quad (i = A, B, C) \tag{12}$$

$$f^L = 0 \tag{13}$$

$$f^\gamma = 0 \tag{14}$$

which will calculate the edge of the ternary eutectic plane in equilibrium with the α and β two-phase region. Other edges of this invariant eutectic plane could be calculated by setting different groups of phases in Eqs. 12–14.

This algorithm for calculating a 3D phase diagram could be easily extended to calculate 3D sections of phase diagrams in a multi-component system with extra constraints on the compositional variables.

CONTOUR DIAGRAM

The concepts of zero-phase fraction and one-phase fraction can be generalized further to construct contour property lines or boundaries. Here, we still use phase fraction as an example.

In some practical applications, we are interested in whether the phase fraction of a specific phase has a value between zero and one. For example, during a heat treatment process of a Ti alloy, if the application requires the fraction of β phase to remain as certain percentage (e.g., 50%), we can calculate the phase fraction contour lines and plot them on the diagram. Figure 4a shows an isoplethal section of Ti-Al-V-N-O with 4 wt.% of V, 0.02 wt.% of N and 0.1 wt.% of O. The amount of Al changes in this isoplethal section. This diagram shows only the phase boundaries, e.g., the phase boundary between β and $\alpha + \beta$ with $f^\alpha = 0$. It does not tell us where the contour line of $f^\beta = 0.5$ actually is. To determine the contour line for a given value of $f^\beta = d$ $(0 \le d \le 1)$ in the two-phase region of $\alpha + \beta$, the following equations must be solved,

$$\mu_i^\alpha = \mu_i^\beta \ (i = \text{Ti, Al, V, N, O}) \tag{15}$$

$$f^\beta = d \quad 0 \le d \le 1 \tag{16}$$

By solving this set of equations with composition constraints on the components of V, N and O, the contour lines with fixed phase fractions of β phase (f^β) can be calculated in the $\alpha + \beta$ phase region,
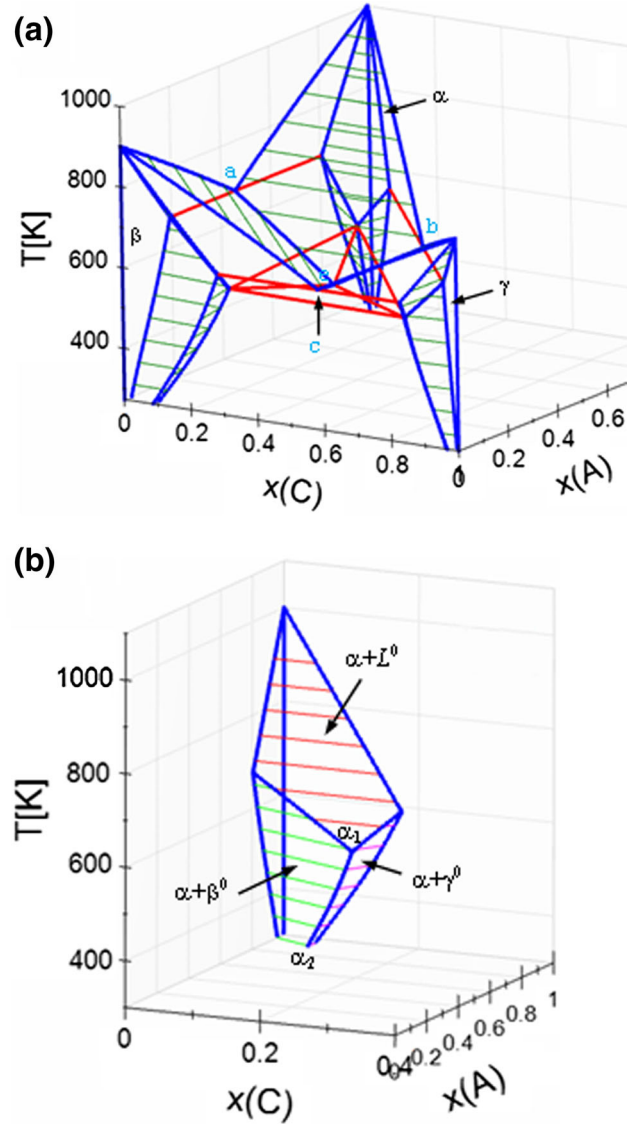

(a)

(b)

Fig. 3. (a) The calculated 3D phase diagram of A–B–C system with isothermal lines (green) and the invariant reactions (red). (b) The 3D surface of α phase with isothermal lines. $\alpha + L^0$ represents the α phase in equilibrium with the liquid phase and $f^L = 0$.

which are shown as the red lines in Fig. 4b. The contour values of f^β are labeled for each line in green. The contour line with $f^\beta = 0.5$ is especially drawn in green to show that this is the line we looked for in this example. This figure shows clearly that the contour lines of a phase fraction are not distributed evenly in a phase region. With the help of Fig. 4b, the heat treatment temperature for a Ti alloy can be easily identified if the Al content is known.

If the constraint of Eq. 16 is replaced by any other property constraint, we should be able to calculate a contour diagram for any property. Another example of density contour diagram will be presented in another paper in this issue of *Journal of Metals*.[21]
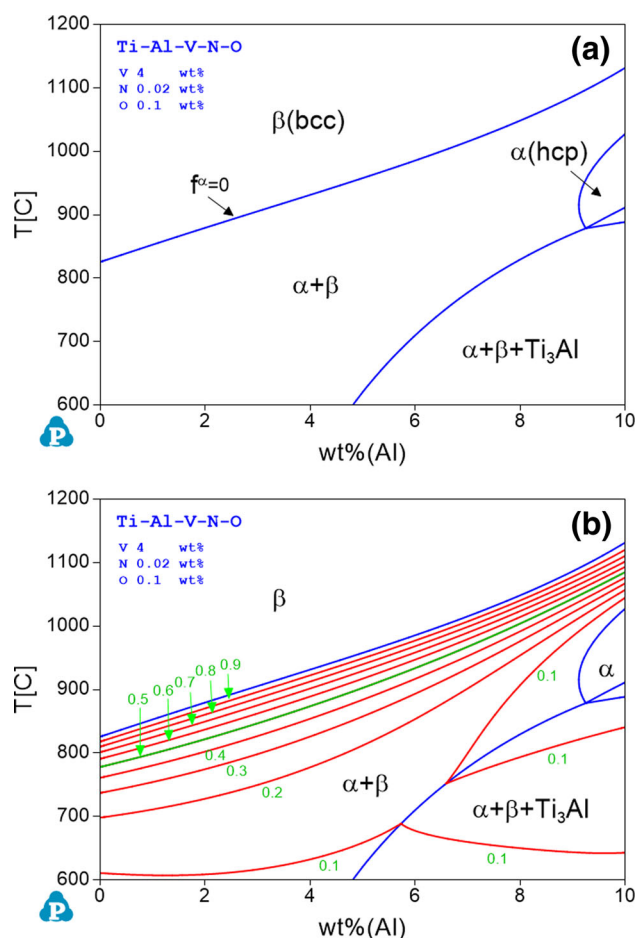
Fig. 4. (a) Calculated isoplethal section of Ti-Al-V-N-O system. (b) Isoplethal section with calculated contour lines of $f^\beta = d$. The value of d is labeled beside the contour line in green.

SUMMARY

Two different types of algorithms have been described: zero-phase fraction algorithm and one-phase fraction algorithm. The zero-phase fraction algorithm is suitable for calculating 2D sectional phase diagrams. The one-phase fraction algorithm can be used for calculating 3D phase diagrams. 3D phase diagrams are usually represented by the univariant lines on phase boundaries and the contour lines on the 3D boundary surfaces. The two types of algorithms have been generalized to calculate a contour line of any property.

REFERENCES

1. J.E. Allison, P. Collins, and G. Spanos (eds.), *Proceedings of the 1st World Congress on Integrated Computational Materials Engineering* (Hoboken: Wiley Inc., 2011).
2. M. Li, C. Campbell, and K. Thornton (eds.), *Proceedings of the 2nd World Congress on Integrated Computational Materials Engineering* (Hoboken: Wiley Inc., 2013).
3. R. Schmid-Fetzer, *J. Phase Equilib. Diff.* 35, 735–760 (2014).
4. M. Hansen, *Constitution of Binary Alloys*, 2nd ed. (New York: McGraw-Hill, 1958).
5. *Handbook of Ternary Alloy Phase Diagrams*, 10 vols., (Materials Park, ASM International, 1995).
6. J.J. van Laar and Z. Phys, *Chem.* 63, 216 (1908).
7. J.J. van Laar and Z. Phys, *Chem.* 64, 257 (1908).
8. J.L. Meijering, *Philips Res. Rep.* 18, 318 (1963).
9. L. Kaufman and H. Bernstein, *Computer Calculation of Phase Diagrams*, (Academic Press, 1970).
10. ASM Handbook, Vol. 3, *Alloy Phase Diagrams*, (Materials Park, ASM International, 1992).
11. *iPandat—Live Phase Diagram*, CompuTherm, LLC. http://ipandat.computherm.com/.
12. *Alloy Phase Diagrams Database*, ASM International. http://www1.asminternational.org/asmenterprise/apd/.
13. *FactSage Online*, C.R.C.T., http://www.crct.polymtl.ca/fact/documentation/.
14. *MIST, Phase Online*, The American Ceramic Society and NIST. http://phase.ceramics.org/publicstore/default.aspx.
15. *CALPHAD*, 33,(2009).
16. G. Eriksson, C.W. Bale, and A.D. Pelton, *J. Chem. Therm.* 67, 63–73 (2013).
17. J.E. Morral and H. Gupta, *Scr. Met.* 25, 393–396 (1991).
18. J.E. Morral and H. Gupta, *J. Chim. Phys.* 90, 421–427 (1993).
19. F.N. Rhines, *Phase Diagrams in Metallurgy* (New York: McGraw-Hill, 1956).
20. *Pandat Software*, CompuTherm, LLC (2015).
21. J. Zhu, C. Zhang, W. Cao, S. Chen, and F. Zhang, *JOM*, (2015). doi:10.1007/s11837-015-1493-6.